Chemical Engineering Journal 512 (2025) 162098

Contents lists available at ScienceDirect

Chemical Engineering Journal

journal homepage: www.elsevier.com/locate/cej

Double-emulsion droplet digital CRISPR/Cas12a for amplification-free, absolute quantification of nucleic acids at attomole levels

Yang Zhang [a], Hangrui Liu [b], Shi-Yang Tang [a,c], Yaxiaer Yalikun [d], Tracie J. Barber [a], Keisuke Goda [e,f,g], Ming Li [a,*]

[a] School of Mechanical and Manufacturing Engineering, University of New South Wales, Sydney NSW 2052, Australia
[b] Department of Bioengineering and Therapeutic Sciences, University of California San Francisco, San Francisco, CA 94158, USA
[c] School of Electronics and Computer Science, University of Southampton, Southampton SO17 1BJ, UK
[d] Division of Materials Science, Nara Institute of Science and Technology, 630-0192 Ikoma, Japan
[e] Department of Chemistry, The University of Tokyo, Tokyo 113-0033, Japan
[f] Department of Bioengineering, University of California, Los Angeles, CA 90095, USA
[g] Institute of Technological Sciences, Wuhan University, Hubei 430072, China

ARTICLE INFO

Keywords:
CRISPR/Cas12a, Droplet microfluidics
Double emulsion droplets
Flow cytometer
DNA quantification

ABSTRACT

The quantification of nucleic acids is of prominent importance for biology and medicine sciences. Droplet digital polymerase chain reaction (ddPCR) provides an absolute measure of target nucleic acid molecules with unrivalled sensitivity and accuracy, but suffers from limitations inherent to PCR amplification, droplet partition, and signal detection. Here, we present an ultrasensitive, rapid, and high-throughput technique for the absolute quantification of nucleic acids without the need for amplification, by combining the double-emulsion (DE) droplet digital platform with CRISPR/Cas12a system (d^3CRISPR). We demonstrate the developed approach by accurately quantifying various DNA molecules, such as target human papillomavirus (HPV) 18, HPV16, and *E. coli* DNA, at concentrations down to attomole levels. This represents an over 1,000-fold improvement in the limit of detection (LOD) compared to existing bulk amplification-free Cas12a assays. Given the versatility and generality of the CRISPR system, we believe that this approach has great potential in the detection and measurements of diverse nucleic acid molecules for many biomedical, clinical, and environmental applications.

1. Introduction

Ultrasensitive quantitative detection of nucleic acids holds great importance in various fields, such as gene expression profiling, pharmacogenomics, personalised medicine, drug development, and molecular diagnostics [1–5]. While quantitative polymerase chain reaction (qPCR) has become the gold standard for nucleic acid analysis [6,7] by monitoring the exponential rise of amplicons, it often exhibits inaccuracy, particularly when detecting low-abundance samples. In contrast, droplet digital PCR (ddPCR) allows absolute quantification of target nucleic acids with unparalleled precision and accuracy. ddPCR partitions samples into millions of discrete, volumetrically defined water-in-oil (W/O) droplets, with each droplet containing either one or no target molecule. The target concentration is determined by measuring the number of droplets that contain target molecules [8]. Despite its advantages, ddPCR has limitations inherent to the PCR amplification process. These include the potential for contamination, the need for well-designed primers, and rigorously controlled thermal cycling procedures [9].

Several isothermal amplification methods, such as loop mediated isothermal amplification (LAMP) [10], rolling circle amplification (RCA) [11], and recombinase polymerase amplification (RPA) [12], have emerged as viable alternatives to PCR. These technologies enable rapid DNA amplification at constant temperatures, reducing dependence on sophisticated instruments and trained personnel [13]. However, they may suffer from limitations, such as reduced specificity, non-specific amplification, and susceptibility to inhibitors [14]. Moreover, amplification-free methods, such as mass spectrometry [15], surface-enhanced Raman spectroscopy (SERS) [16], and fluorescence in situ hybridization (FISH) [17–19], have been explored for nucleic acid quantification in droplet digital assays. Despite their favourable features, these methods face challenges, such as limited sensitivity and the

* Corresponding author.
E-mail address: ming.li3@unsw.edu.au (M. Li).

https://doi.org/10.1016/j.cej.2025.162098
Received 2 January 2025; Received in revised form 13 March 2025; Accepted 27 March 2025
Available online 2 April 2025

need for substantial sample volumes to mitigate amplification-related biases [18,19]. These hurdles underscore the need for new approaches capable of achieving PCR-like sensitivity while avoiding amplification-related biases [20].

Clustered regularly interspaced short palindromic repeats (CRISPR)-based techniques present a promising avenue to address this unmet need [21]. Upon crRNA-mediated binding to a target nucleic acid [22–24], Cas12a *trans*-cleaves single-stranded DNA (ssDNA) reporters to release fluorescence signals, enabling rapid and high-efficiency target detection [25–27]. Recent research has explored the integration of droplet digital platforms with CRISPR/Cas systems for nucleic acid quantification in unamplified samples [28–33]. Nevertheless, previous studies primarily used W/O single emulsion (SE) droplets for sample partitioning, which exhibited unsatisfactory stability and uniformity [34]. Additionally, detection methods relying on fluorescence imaging introduced external errors, thus limiting quantification precision [35]. In contrast, water-in-oil-in water (W/O/W) double emulsion (DE) droplets have demonstrated robust stability and reliable compartmentalization [36]. Furthermore, DE droplets suspended in an aqueous solution are compatible with commercially available flow cytometry (FC) [37–39], enabling high-throughput, high-precision, and ultrasensitive quantification and classification of droplet partitions [40]. These features make DE droplets well-suited for digital CRISPR-based assays. However, to date, no digital assay utilizing DE droplets for the absolute quantification of nucleic acids has been reported.

In this study, we report a **d**ouble-emulsion **d**roplet **d**igital **CRISPR**/Cas12a (d^{3}CRISPR) technique for the absolute quantification of nucleic acids without the need for amplification. Using human papillomavirus (HPV) 18 DNA as a model target, we optimized Cas12a/crRNA reaction conditions within DE droplets to enhance their fluorescence intensity. We conducted a comprehensive evaluation of d^{3}CRISPR for sensitivity, selectivity, and specificity, demonstrating its utility for precise analysis of complex samples with low-concentration target DNA. The d^{3}CRISPR technique is capable of directly quantifying target HPV 18 DNA at the 100 aM level, representing over a 1,000-fold improvement in the LOD compared to existing bulk amplification-free Cas12a assays. To further assess its applicability to real-world samples, we successfully detected and quantified large-sized *E. coli* O157:H7 DNA at the single-molecule level (60 copies/μL) in raw samples. The developed d^{3}CRISPR technique shows great promise in the absolute quantification of different types of nucleic acids across various fields, leveraging the programmability of the Cas12a/crRNA system.

2. Results and discussion

2.1. Workflow of d^{3}CRISPR for absolute DNA quantification

Current strategies mainly focus on amplifying target molecules to increase signal levels, particularly for low-abundance samples. In this study, we utilize a single target molecule to interact with massive fluorescence reporters in DE droplet partitions for DNA quantification without upstream pre-amplification of the target. As illustrated in Fig. 1, a one-pot reaction system containing Cas12a, CRISPR RNA (crRNA), target double-stranded DNA (dsDNA), and single-stranded DNA (ssDNA) reporter is mixed in nuclease-free water (NFW). To prevent widespread activation of Cas12a before encapsulation within DE droplets, we place the reaction sample on ice and rapidly load it into a microfluidic chip (see **Fig. S1**) as the inner phase solution. The sample is partitioned into numerous discrete DE droplets by an intermediate oil phase, with an outer aqueous phase, which are then collected in a centrifuge tube and

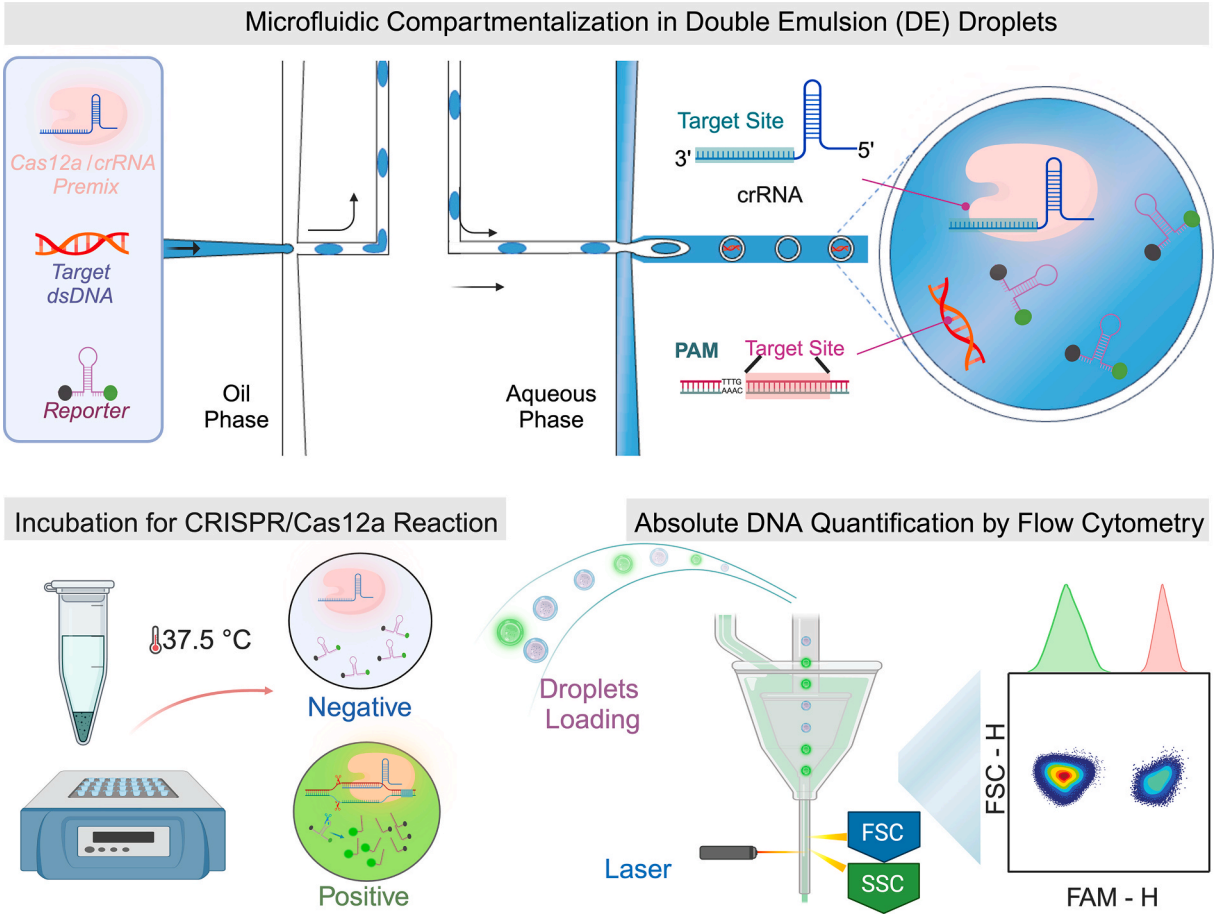

Fig. 1. Schematic illustration of double-emulsion droplet digital CRISPR/Cas12a (d^{3}CRISPR) technique for amplification-free, absolute DNA quantification.

incubated at a constant temperature (e.g., 37.5 °C).

During this incubation period, the programmed crRNA recognizes and unwinds the target dsDNA containing a protospacer adjacent motif (PAM). This exposes the active site of the RuvC nuclease in Cas12a, which then non-specifically cleaves surrounding quenched ssDNA reporters, releasing a fluorescent signal. Since a single activated Cas12a molecule can cleave nearly 1,000 ssDNA reporters, fluorophores can be effectively accumulated and retained within droplets (known as positive droplets). Conversely, in the droplets without target DNA (negative droplets), Cas12a remains inactive, and no fluorescent signal from the reporters is released. Following incubation, FC is employed to determine the concentration of target DNA in the original sample by accurately and rapidly counting the number and the fraction of positive droplets.

Additionally, the size of the droplets and the sample concentration are controlled to ensure that almost all droplets contain either 0 or 1 target DNA molecule, according to the Poisson distribution. The obtained fraction of positive droplets (FPD) can be used to determine the target concentration C using the following relationship: $C = \frac{1}{V}\ln\frac{1}{1-FPD}$, where V is the average volume of the DE droplets. Compared to existing quantification strategies, d^{3}CRISPR technique can accurately determine the absolute quantity of specific nucleic acid molecules in an unamplified sample. This significantly reduces the complexity, time, and cost associated with nucleic acid-based detection.

2.2. Optimization of reaction conditions for signal enhancement

Enhancing the signal of target molecules to detectable levels is crucial for detecting low-concentration or rare target molecules in samples by droplet digital assays. Enhanced signals are easier to distinguish from background noise and can reduce errors caused by variations in experimental conditions, thus improving detection accuracy and sensitivity. Furthermore, signal enhancement can expand the

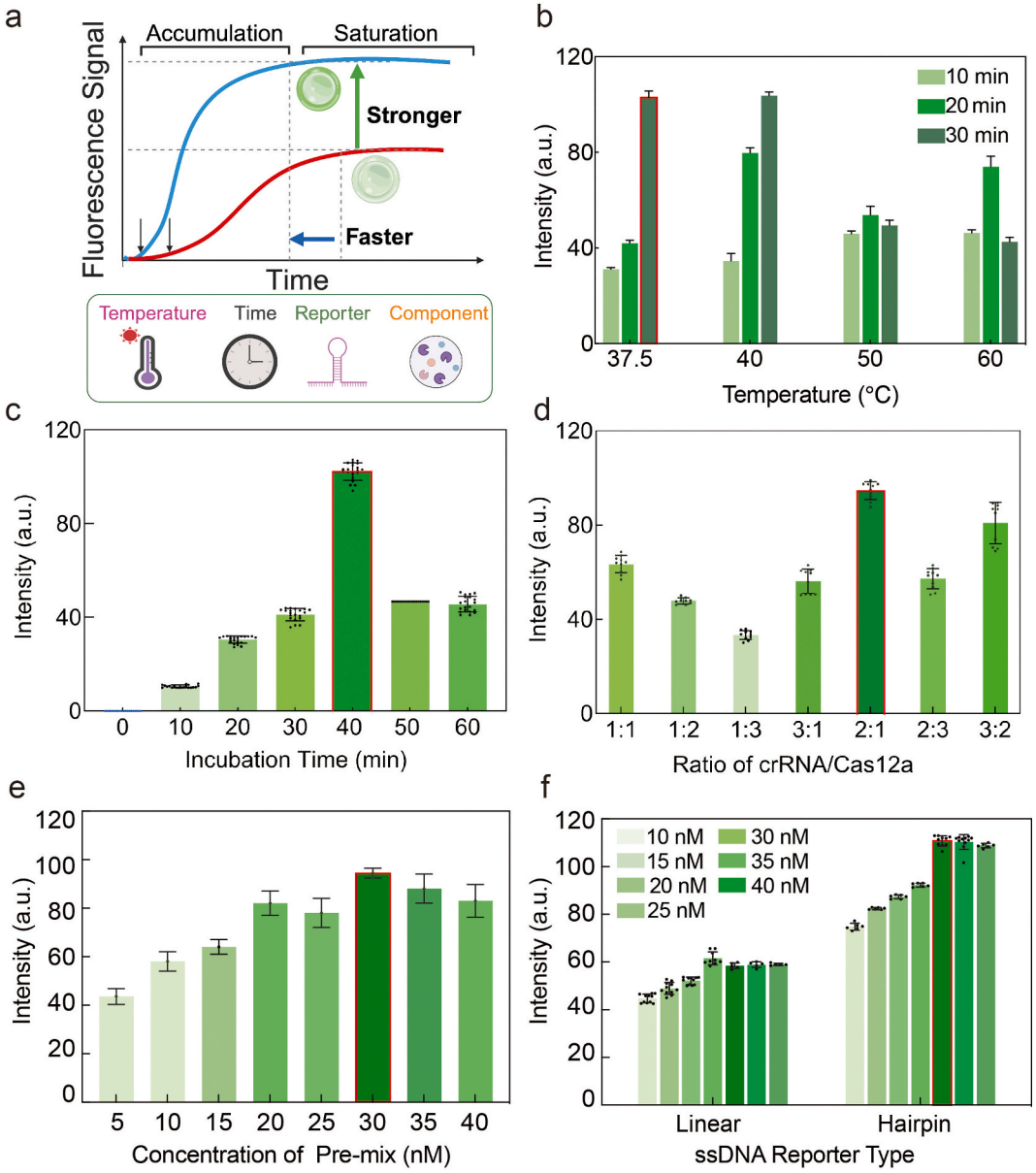

Fig. 2. Optimization of the CRISPR/Cas12a reaction in DE droplets. (a) The efficiency of CRISPR/Cas12a assay in droplets is optimized by monitoring the fluorescence intensity of positive droplets. The effects of (b) temperature, (c) incubation time, (d) the ratio of crRNA to Cas12a, (e) the concentration of Cas12a/crRNA premix, and (f) the type and concentration of reporters on the end-point fluorescence intensity of positive droplets are examined and compared. Data are represented as mean ± standard error of the difference between means of 100 droplets. The assays are conducted by detecting 10 fM target HPV 18 DNA. The selected optimal condition is highlighted in the red box. (For interpretation of the references to colour in this figure legend, the reader is referred to the web version of this article.)

dynamic range of detection, enabling simultaneous detection of both low and high concentrations of target molecules, thereby providing a more comprehensive understanding of the target content in samples. To achieve optimal signal output, we optimized key factors of the CRISPR/Cas12a system, including reaction temperature, incubation time, the ratio of each component in the reaction mixture, and the type of reporter (see Fig. 2**a**). It is worth noting that, to the best of our knowledge, this study is the first to optimize the CRISPR/Cas12a reaction system inside droplets. There are differences between microdroplet and bulk-solution reactions, particularly in terms of sample volume and target molecule concentration. More importantly, some molecules may be lost during reagent mixing, droplet encapsulation, or the analysis process, leading to variations in capture efficiencies and signal intensity.

First, we set a temperature range from 37.5 to 60 °C and incubated the DE droplets (~30 μm) encapsulating with the CRISPR/Cas12a reaction and 100 fM target HPV 18 DNA for 10, 20, and 30 min, respectively. It can be clearly seen from Fig. 2**b** that at temperatures of 37.5 and 40 °C, with an incubation time of 30 min, the fluorescence intensity of positive droplets is almost equal and significantly higher than under other conditions. Therefore, we determined the optimal incubation temperature to be 37.5 °C. Next, to further determine the optimal reaction time, we incubated the droplets at a constant temperature of 37.5 °C for different durations. The droplet fluorescence intensity was found to be highest at 40 min of incubation (Fig. 2c). We found that incubation times longer than 40 min limit the *trans*-cleavage activity of Cas12a. This is likely due to the accelerated diffusion of cleaved fluorescent reporter fragments into the surrounding aqueous phase as the incubation time progresses [41,42]. Moreover, fluorescent molecules gradually decay over time due to exposure to light and heat. These factors contributed to a decrease in the overall fluorescence intensity of the droplets.

Moreover, we mixed crRNA and Cas12a at different concentration ratios while keeping other components constant. Using the optimized incubation conditions (37.5 °C, 40 min), we found that the fluorescence intensity of positive droplets was strongest when the ratio of crRNA to Cas12a was 2:1 (Fig. 2**d**). Subsequently, we investigated the effect of the Cas12a/crRNA premix concentration using Cas12a concentrations ranging from 5 to 40 nM and crRNA concentrations ranging from 10 to 80 nM, while maintaining the optimal 2:1 crRNA: Cas12a ratio. As shown in Fig. 2e, the fluorescence intensity was highest at a premix concentration of 30 nM compared to the other concentrations. We also examined the influence of reporter types and concentrations on the fluorescence intensity of positive droplets. Two different reporters, the single-strand hairpin reporter and conventional linear ssDNA, were used. The results (Fig. 2**f**) showed that the signal intensity of positive droplets emitted by hairpin reporters was nearly twice as high as that emitted by the linear reporter. Our findings are supported by experimental testing in bulk (**Fig. S2**) and align with previous studies [43], which show that hairpin reporter exhibits significantly faster and improved fluorescence signal transduction compared to conventional linear ssDNA reporter, due to its superior quenching efficiency and low fluorescence background. The optimal concentration of the hairpin reporter was set at 35 nM, as further increase in concentration did not result in a noticeable increase in droplet fluorescence intensity.

2.3. Quantitative detection of HPV 18 DNA

After optimizing the reaction conditions, we investigated the absolute quantification of target HPV 18 DNA in unamplified samples. To ensure single-molecule encapsulation, we generated DE droplets exhibiting high size uniformity and stability both before and after incubation (**Fig. S3**). Moreover, 100 μL of the sample could be encapsulated in millions of pico-sized DE droplets, and approximately 100,000 DE droplets have been analyzed. This also reduces background noise and false-positive droplets during subsequent detection by FC, thereby minimizing errors in the results.

Using d^{3}CRISPR, one single molecule is sufficient to "light up" a droplet, allowing us to measure the quantity of single DNA molecules by counting each positive droplet as "one" and each negative droplet "zero" (Fig. 3**a**). FC can successfully select DE droplets from all the events detected using an appropriate gating strategy. We optimized the settings, including laser gains, flow rate, scatter thresholds (see **Table S1**), resulting in an overall increase in DE droplet throughput of over 20 % (**Fig. S4**). We evaluated the performance of d^{3}CRISPR using target HPV 18 DNA at five different concentrations:100 aM, 1 fM, 10 fM, 100 fM, and 0.5 pM. After incubation at 37.5 °C for 40 mins, the fraction of positive droplets (FPD) was obtained by both fluorescence imaging and FC (Fig. 3**b**). We compared the FPD values obtained from imaging and FC methods with the theoretical values calculated using the Poisson distribution (Fig. 3**c**). The results showed that the FPDs measured by the FC were significantly closer to the theoretical values and had smaller errors, while the imaging method exhibited relatively larger variations, especially at low concentrations ($< 10^4$ aM).

Additionally, the FPDs were used to calculate the target concentration using the Poisson distribution. Due to the ultrasensitive and precise accounting ability of FC, the measured concentration precisely correlated with the input target HPV 18 DNA concentrations, exhibiting an excellent linear relationship ($R^2 > 0.99$) over a dynamic range from 10^2 aM to 5×10^5 aM (Fig. 3**d**). It's worth noting that, although FPDs and target concentrations can also be obtained by fluorescence imaging, this method typically results in relatively large errors, due to operator subjectivity and image interference. Analysing images of low-abundance samples may lead to missing a small proportion of positive droplets. In contrast, FC counting avoids the effects of human error and background noise, enabling ultra-precise, ultra-fast, and ultra-sensitive counting of DE droplets based on fluorescence intensity.

2.4. Specificity, selectivity, and sensitivity of d^3 CRISPR

We further evaluated the specificity, selectivity, sensitivity of d^{3}CRISPR. We first used a sample containing target HPV 18 DNA with a concentration of 10fM, ensuring each droplet contained at least one target DNA molecule. There results showed an approximately 7-fold increase in fluorescence signal intensity between reactions with the complete components and those without (Fig. 4**a**). Next, we evaluated the specificity of the Cas12a/crRNA system for recognizing specific target DNA sequences. Considering that the Cas12a system can tolerate one or two mismatches in the crRNA spacer sequences, we encapsulated six different types of crRNAs (crRNA$_{18}$, crRNA$_{16}$, crRNA$_{12}$, crRNA$_{20}$, crRNA$_{40}$, and crRNA$_{55}$) with their corresponding target DNA sequences, including high-risk HPV 18 and HPV 16, and low-risk HPV 12, HPV 20, HPV 40, and HPV 55. These sequences belong to the same family but differ by several nucleotides. The orthogonal testing results demonstrated successful discrimination and ultralow cross-reactivity (Fig. 4**b**), indicating that the Cas12a/crRNA system in DE droplets has excellent specificity for discriminating homologous sequences, even those with minimal nucleotide differences.

To further assess the accuracy of d^{3}CRISPR for target DNA quantification in complex samples, we prepared four samples by adding 10 fM of target DNA to a medium containing 20 fM of various HPV DNAs (types 12, 20, 40, 55). Moreover, HPV 16 was introduced as an interfering variable, with 10, 20, 30, 40 fM of HPV 16 were added to the four respective groups of samples. Quantitative tests using d^{3}CRISPR were replicated at least three times for the control sample containing only HPV 18 and for each of the four groups of samples. The FPD values and corresponding measured concentrations of HPV 18 DNA were presented in Fig. 4**c**, yielding average concentration values of 9.50 fM, 19.74 fM, 29.47 fM, and 39.32 fM, respectively. These results closely matched the expected input concentrations. Similarly, we quantitatively analyzed samples containing HPV 16 DNA at concentrations ranging from 10^2 to 10^6 aM. The FPDs of each sample were measured using d^{3}CRISPR (Fig. 4**d**), which were then used to obtain target concentrations via

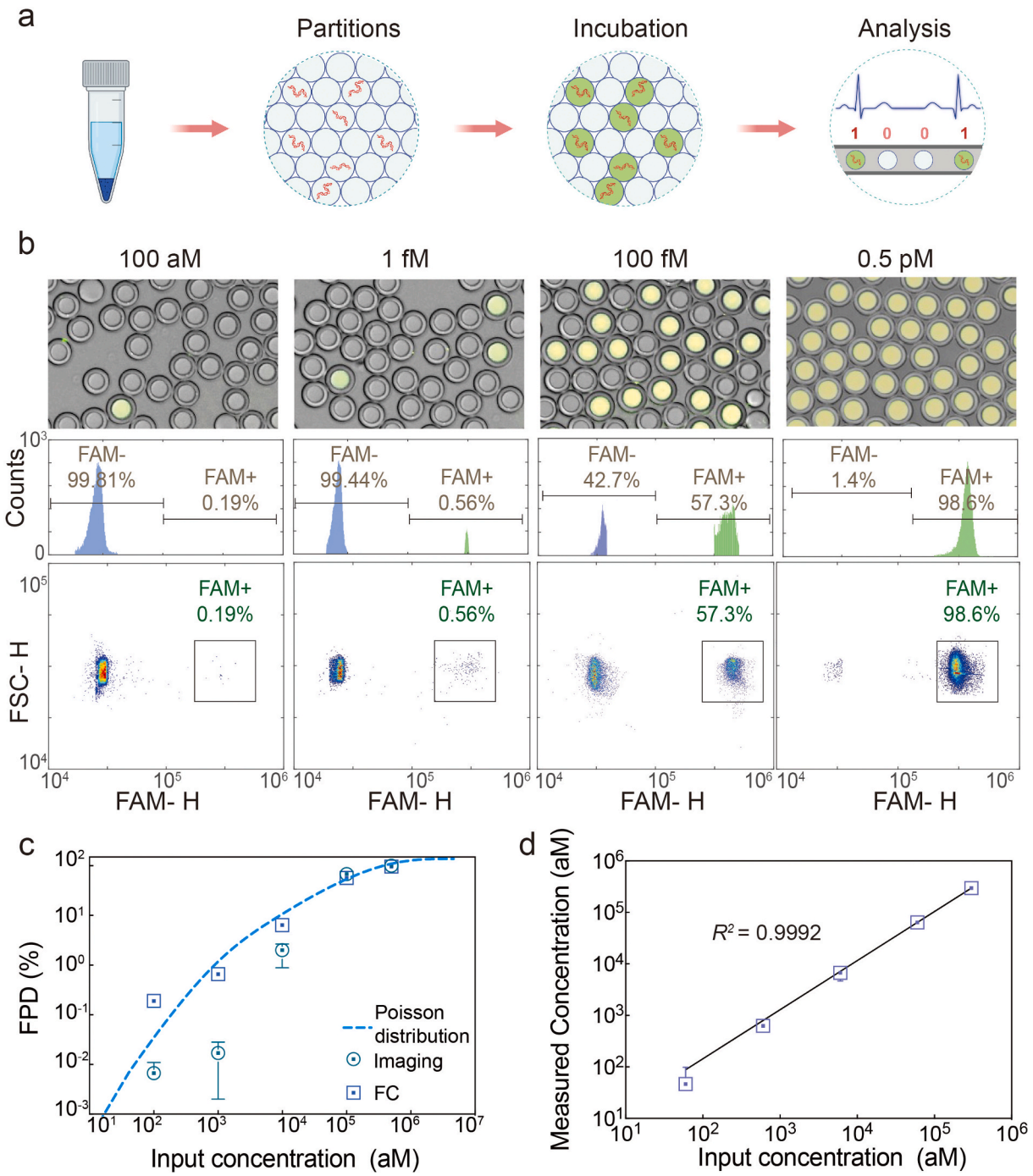

Fig. 3. Absolute quantification of HPV 18 DNA in unamplified samples using d^3 CRISPR. (a) Schematics showing the principle of d^{3}CRISPR for absolute DNA quantification. (b) Brightfield and fluorescence composite imags and FC screening results of DE droplets after incubation. DE droplets containing target HPV 18 DNA at four different concentrations, 100 aM, 1 fM, 100 fM, and 0.5 pM, were analyzed. Scale bar is 50 μm. (c) Comparison of FPD values measured from imaging and FC with those obtained through Poisson distribution calculation. (d) The linear correlation between the measured and input target concentrations (R^2 = 0.9992). The light-coloured areas are the 95 % confidence interval bands indicating the likely location of the true curve.

Poisson distribution. As shown in Fig. 4**e**, the actual quantification results of HPV 16 were consistent with input concentrations, demonstrated an excellent linear correlation (R^2 = 0.9987). These results highlight the high selectively and accuracy of our d^{3}CRISPR approach, even in the presence of potential interferents, and confirm its compatibility for quantifying different target DNAs.

2.5. Quantitative detection of E. coli O157:H7 DNA

To further verify the applicability of our d^{3}CRISPR technique to other real-world samples, we applied it to detect large-sized target DNA from *Escherichia coli* O157:H7. This strain is a highly pathogenic serotype of Shiga-toxin-producing *E. coli* (STEC), a foodborne origin that poses a severe public health threat and incurs significant societal costs. The relatively large size of the target DNA from *E. coli* O157:H7 makes it a suitable model for validating the capability of d^{3}CRISPR to detect a wider range of DNA types. We designed crRNA specifically for target *E. coli* O157:H7 DNA (Fig. 5**a**) and used d^{3}CRISPR to measure target DNA with serially diluted known concentrations. Both fluorescence imaging (Fig. 5**b**) and FC screening (Fig. 5**c**) successfully distinguished

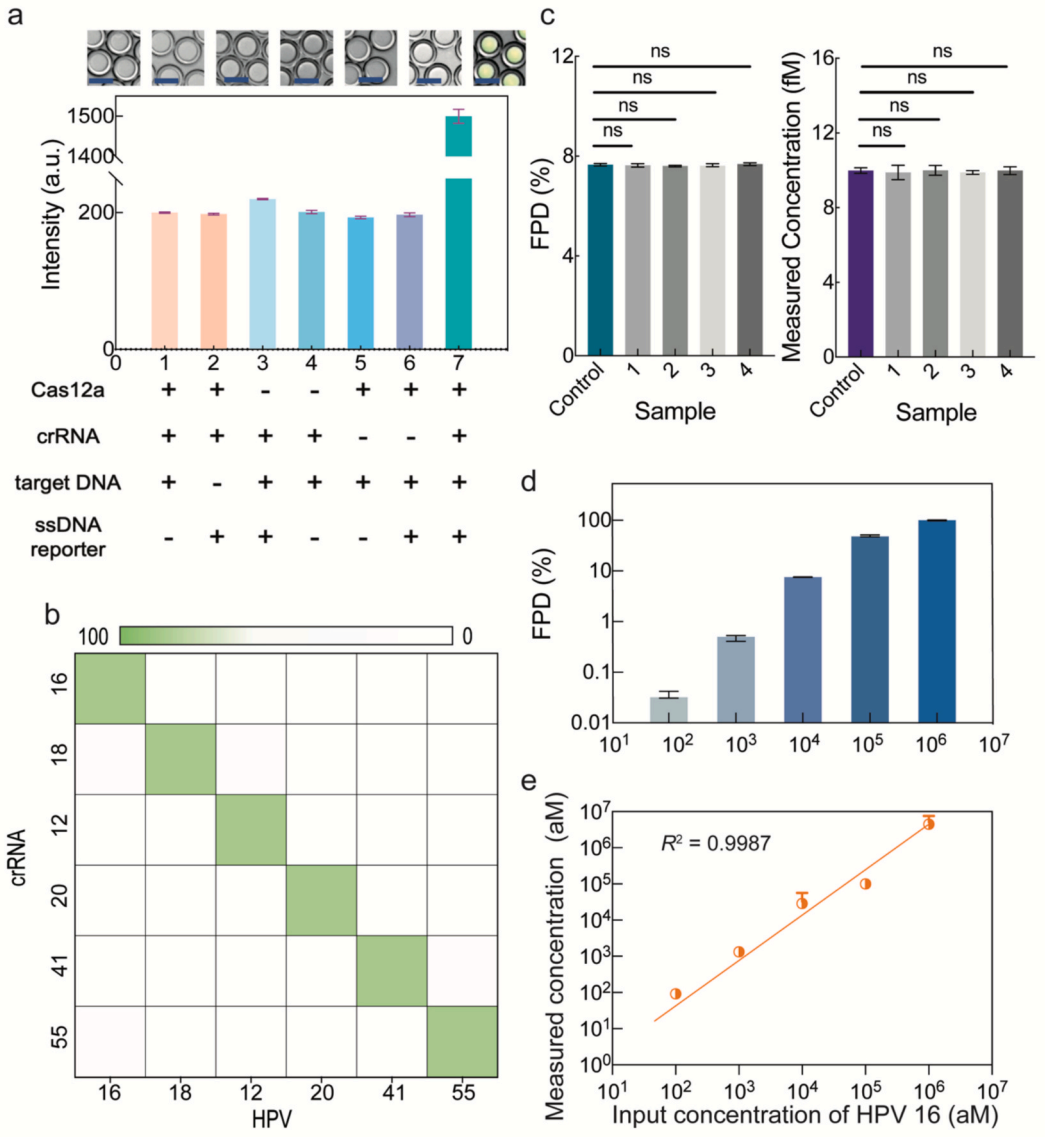

Fig. 4. Evaluation of the specificity, selectivity, sensitivity of d^3 CRISPR. (a) DE droplets containing CRSIPR/Cas12a reactions with various components are imaged after incubation. (20 × magnification, scale bar: 20 μm). (b) Heatmap of fluorescence intensity as a function of crRNA and HPV DNA sequencies. (c) Measured FPDs (left) and concentrations (right) of target HPV 18 DNA in complex samples containing interferents. (d) FPDs measured by d^{3}CRISPR when quantifying samples containing HPV 16 DNA with concentrations ranging from 10^2 to 10^6 aM. (e) The linear correlation between the measured and input target HPV16 concentrations ($R^2 = 0.9987$). Each experiment was repeated three times.

positive droplets containing target DNA in each sample (see **Fig. S5**), with FPD increasing with the concentration of target DNA. The results demonstrated a reproducible LOD down to approximately 60 copies/μL and an excellent linear relationship ($R^2 = 0.9988$) between the input target concentration and FPD (Fig. 5**d**), covering 4 orders of magnitude from 60 to 600,000 copies/μL.

As *E. coli* is known to proliferate in raw food and cause infections in the human body, we further assessed the performance of d^{3}CRISPR for detecting *E. coli* O157:H7 DNA in milk and artificial urine. Target DNA with known concentrations ranging from 100 aM to 100 fM were spiked into milk medium and artificial urine, with a total volume of 50 μL per sample. The quantitative results (Fig. 5**e**) showed a linear relationship (milk: $R^2 = 0.9977$; urine: $R^2 = 0.9971$) between FPD and concentration over the whole range (approximately 60 to 600,000 copies/μL). The linear fit for milk samples was slightly worse than those in PBS and urine, primarily due to higher background noise and opacity in the milk matrix.

According to the FPD versus concentration curve (see **Fig. S6**), if droplet size remains constant, the calculated FPD at concentrations below 100 aM approaches zero. This indicates that the likelihood of target DNA being encapsulated within a droplet and subsequently detected becomes negligible. Therefore, we define our LOD as 100 aM. To further reduce the LOD, a potential approach would be to generate larger DE droplets. This would increase the partition volume and enhance the probability of capturing ultra-low-abundance molecules. It is important to note that current Cas12a-based assays for DNA quantification without amplification typically achieve a limit of detection (LOD) of approximately 100 fM (approximately 60,000 copies/μL). In contrast, our d^{3}CRISPR technique achieved a remarkable improvement, providing over a 1,000-fold enhancement in LOD compared to previous bulk CRISPR assays (see **Table S4**).

To further evaluate the quantitative capability of d^{3}CRISPR in detecting real samples, we prepared five milk samples contaminated with *E. coli* O157:H7 at different concentrations and directly quantified

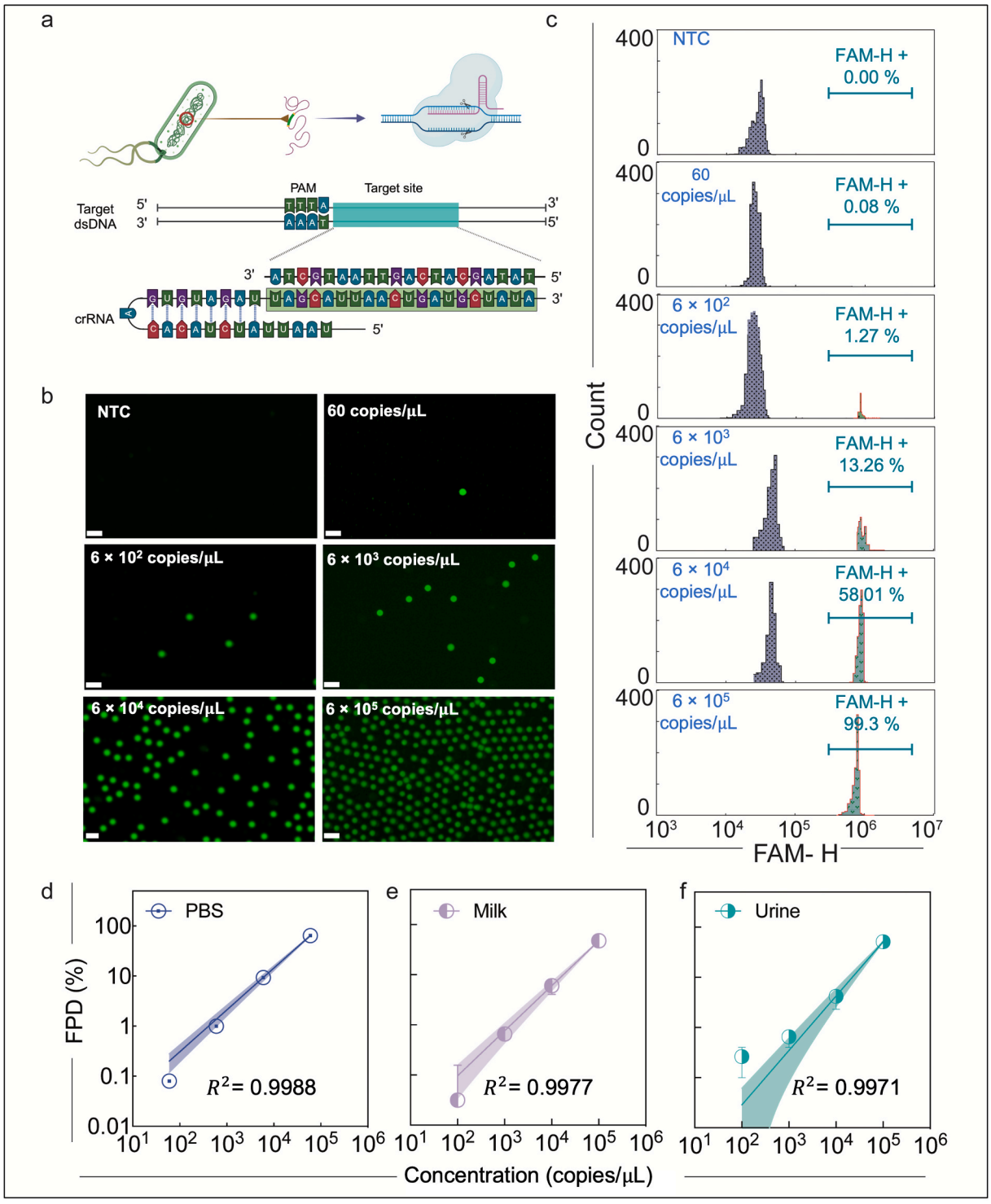

Fig. 5. Quantitative detection of *E. coli* DNA using d[3]CRISPR. (a) Schematic illustration of the Cas12a/crRNA system matching with target DNA. The pre-designed crRNA is provided in detail with the PAM sequence and dsDNA target site (highlighted in blue). (b) End-point fluorescence images of DE droplets containing 0 (NTC), 60, 600, 6000, 60000, and 600,000 copies/µL of *E. coli* DNA (20 × magnification, scale bar: 50 µm); (c) Histograms of fluorescence intensity of negative and positive (highlighted in green area) DE droplets containing target DNA of different concentrations obtained by FC. FPDs for each sample concentration are presented in red. (d-f) The linear relationship between input DNA concentration and measured FPD in (d) PBS, (e) diluted milk, and (f) artificial urine. The light-coloured areas are the 95 % confidence interval bands indicating the likely location of the true curve. (For interpretation of the references to colour in this figure legend, the reader is referred to the web version of this article.)

extracted complete genomic DNA. Since the exact concentrations of these DNA samples were unknown, we performed standard qPCR quantification in parallel to provide a reference measurement, as shown in **Fig. S7**. The concentrations measured by both methods showed a similar trend in target DNA quantification across different samples (see **Fig. S8**). Paired t-tests were performed to analyze the statistical significance between two methods and there was no statistically significant difference in the concentrations measured by the two methods across all

five samples.

It is important to note that the complexity of the real sample matrix and the presence of complete genomic DNA introduced additional challenges to CRISPR-based detection, potentially affecting assay precision. The presence of cellular debris, nucleases, and other biological components may have impacted Cas12a activity, potentially affecting assay precision by increasing non-specific cleavage or reducing *trans*-cleavage efficiency. Moreover, the variability in real sample compositions, along with potential inhibitors such as proteins, polysaccharides, or metal ions, may have interfered with Cas12a recognition, contributing to higher measurement errors across replicates [44]. However, despite these variations, the overall trend of measured concentrations aligned well between our d^{3}CRISPR method and standard qPCR.

3. Discussion

CRISPR/Cas12a-based nucleic acid detection has demonstrated significant potential in molecular diagnostics, particularly through its combination with isothermal amplification techniques, as seen in commercialized assays like SHERLOCK and DETECTOR. While isothermal amplification enhances target molecule concentration, enabling high sensitivity, it also presents limitations, including susceptibility to nonspecific amplification and background noise, which can compromise detection. In response to the growing demand for precision and streamlining in nucleic acid detection, our proposed d^{3}CRISPR approach, based on the combination of droplet digital assays and FC screening, offers a rapid, ultra-sensitive, and high-throughput method for absolute nucleic acid quantification without relying on amplification.

The highly efficient *trans*-cleavage activity of Cas12a, capable of cleaving surrounding ssDNA reporters at a high ratio (over 1:10^3), eliminating the need for target DNA pre-amplification. Additionally, by partitioning the bulk sample into millions of miniaturized droplet compartments (~50 μL each), reagent consumption and reaction volumes can be minimized, making the assay suitable for detecting low-abundance target DNA in small-volume clinical samples. The d^{3}CRISPR assay, under optimal reaction and incubation conditions, resulted in a significant increase in fluorescence signal (over 10^4-fold) compared to bulk samples. This signal enhancement facilitates easy differentiation between positive and negative droplets, enabling accurate absolute quantification of target DNA.

The integration of CRSIPR/Cas12a-based assays with droplet digital platform also holds promise for developing point-of-care diagnostic devices for biomarker quantification. Through experimental validation, d^{3}CRISPR approach demonstrates single-molecule analytical sensitivity (at aM levels) with a dynamic range spanning 5 orders of magnitude, which covers the natural range for DNA expression. Additionally, d^{3}CRISPR shows broad applicability in quantifying different DNA molecules (e.g., HPV DNA and *E. coli* DNA) in various media, yielding reliable results.

Despite the significant advantages of d^{3}CRISPR technique, there are a few limitations. First, it cannot directly quantify targets in high-concentration samples. When the concentration of target DNA reaches 1 pM, all droplets (~ 14 pL each) contain at least one target molecule, making sample concentration measurement impossible. However, this issue can be addressed by diluting the initial samples by a known factor. In addition, although DE droplets can maintain superior stability and robust partitions than SE droplets, their generation process is relatively complicated. Nevertheless, this issue can be mitigated by adopting simpler and faster DE droplet generation methods like vortex [45] and ultrasound activation [46]. Furthermore, the use of FC requires laboratory conditions and professional operation, making it unsuitable for point-of-care testing (POCT) applications [47,48]. Fortunately, alternative integrated on-chip detection techniques, such as flow cytometry with microlens arrays [49] and portable 3D fluorescence imaging flow cytometry [50], could enable the development of more user-friendly and portable devices [51].

4. Methods and materials

4.1. CRIPSR/Cas12a assay

EnGen® Lba Cas12a was purchased from Integrated DNA Technologies, Inc (USA). All sequences of CRISPR related RNA (crRNA), HPV 18 DNA, *E. coli* O157:H7 DNA and FQ reporters in this study, listed in **Table S2**, were synthesized by New England Biolabs (UK). UltraPure™ DNase/RNase-Free Distilled Water (NFW) was purchased from (10977015, Thermo Fisher Scientific, Waltham, MA, USA). All purchased nucleic acid oligos (in **Table S3**) were delivered in solution (normalized to 100 μM in IDTE buffer, pH 8.0). NEBuffer™ r2.1 was purchased from New England Biolabs (UK).

4.2. Microfluidic chip fabrication

The Poly(dimethyl)siloxane (PDMS)-glass microfluidic chip for DE droplet generation is designed using AutoCAD (Autodesk, CA). After design, the original pattern was transferred onto a 3-inch silicon wafer to create a mold by a direct-write optical lithography machine (MicroWriter ML3, Durham Magneto Optics, Durham, UK). The mold consists of two layers: a shallow channel with a height of ~ 15 μm and a width of ~ 23 μm, which serves as a hydrophobic W/O SE droplet generator, and a deeper channel with a height of ~ 25 μm and a width of ~ 30 μm, which functions as a hydrophilic DE generator. The shallow and deep microchannels were made of SU-8 3010 and SU-8 3025, respectively (MicroChem, Newton, MA, USA). PDMS microchannel was fabricated via standard soft photolithography, and spatial patterning of wettability in the microchannel was created using the method comprehensively described in our previous study [39].

4.3. DE droplet generation

The proposed two-layer microfluidic device for DE droplet generation consists of three inlets for injecting inner, middle, and outer phases and one outlet for collection. The components for each phase are detailed as follows: the inner phase is CRISPR/Cas12 reaction containing Cas12a, crRNA, ssDNA reporter, target dsDNA, 1 × NEBuffer, NFW; the middle phase is composed of Bio-Rad droplet generation oil for probes (1863005, Bio-Rad, Hercules, CA, USA); and the outer phase consists of 2 % w/v Pluronic-127 and 2 % v/v Tween 20 (P9416, Sigma-Aldrich, St. Louis, MO, USA) in 1 × phosphate-buffered saline (PBS, 10010023, Thermo Fisher Scientific, Waltham, MA, USA). For successful FC screening of DEs, the outer diameter (OD) of the generated DE droplets is ~ 30 μm, which is less than 1/4 of nozzle size (120 μm). The inner core diameter (ID) is about 25 μm, encapsulating one-pot CRISPR/Cas12a reaction with samples containing target DNA molecules of various concentrations.

4.4. CRISPR/Cas12a reaction optimization

We prepared a 50 μL CRISPR/Cas12a reaction containing 20 nM Cas12a, 25 nM crRNA, 50 nM ssDNA reporter, 1 × NEBuffer™ r2.1 (NEB #B9200, NEW ENGLAND Biolabs, UK), and 30 μL NFW to optimize incubation time and temperature. To investigate the effect of the ratio of crRNA and Cas12a, crRNA and Cas 12a with various concentrations (crRNA: 20, 40, 60 nM; Cas 12a: 6.7, 10, 30, and 13.3 nM) were added into the above reaction. After incubating for 40 min at 37.5 ℃, the fluorescence intensity of each group of droplets was measured. Next, we prepared a 100 nM Cas12a and crRNA premix by mixing stock Cas12a and crRNA in NFW at room temperature for 15 min. The prepared premix was then diluted into Cas12a reaction to obtain different concentration gradients. For comparing the effects of linear ssDNA reporter and hairpin reporter, 50 μL of reaction mixtures were prepared, each

including 30 nM premix, 50 nM ssDNA reporter, 5 μL 1 × NEBuffer™ r2.1, 100 nM target HPV 18 dsDNA, and NFW.

4.5. Fluorescence imaging

Approximately 10 μL of DE droplets after incubation were transferred onto a glass slide using a pipette. The fluorescence images of DE droplets were captured using an inverted fluorescence microscope (Olympus IX83, OLYMPUS, Tokyo, Japan) with a digital camera (DP74, OLYMPUS, Tokyo, Japan). Fluorescence images were taken with excitation by blue light (488 nm) at an intensity of 0.06 kW/cm^2, with an exposure time of 30 ms for each image. The diameter and fluorescence intensity of each droplet was measured and calculated by ImageJ (National Institute of Health, MD, USA).

4.6. Flow cytometry (FC) data acquisition and analysis

All collected DE droplets were resuspended in 100 μl of outer phase solution in the wells of a 96-well plate. A flow cytometer CytoFLEX (Beckman Coulter Life Sciences, Miami, FL, USA) was used to quantitatively analyze DE droplets with a 488 nm excitation laser and a FITC (λ_{ex} = 488 nm/λ_{em} = 525 nm) bandpass filter. Importantly, extraneous scatters markedly decreased, indicating fewer droplet breakage events and less free oil drop loading into the pipeline. Data from FC was acquired by CytExpert 2.4 (Beckman Coulter Life Sciences, Miami, FL, USA) and processed by a commercial software FlowJo (FlowJo v10, TreeStar, Ashland, OR, USA). Statistical analysis plots were produced by Prism 10.0 (GraphPad Software, LLC, BOSTON, USA) and MATLAB (The MathWorks, Inc., CA, USA).

4.7. E. coli O157:H7 DNA sample preparation

Normal skimmed milk (Coles group Ld. VIC, Australia) was diluted in NFW at a ratio of 1:10. Serial dilutions of samples containing target *E. coli* O157:H7 DNA were prepared by spiking DNA solutions in the prepared milk to achieve concentrations ranging from 1fM to 500 fM. The mixture was vortexed digitally to ensure uniform distribution of target DNA molecules. Similarly, urine samples containing target DNA at different concentrations were obtained by replacing the diluted milk with artificial urine (SAE0074, Sigmatrix Urine Diluent, Sigma-Aldrich, St. Louis, MO, USA).

4.8. Bacterial culture and harvesting

A single colony of *Escherichia coli* (*E.coli*) O157:H7 was cultured in Luria-Bertani (LB) broth supplemented with kanamycin (50 μg/mL) overnight at 37 °C for 16 h at 200 rpm. Afterward, 1 mL of skim milk (Coles group Ld. VIC, Australia) was inoculated with different amounts of the bacterial culture, mixed well, and incubated at 37 °C for 4 h to allow bacterial growth. Then, 500 μL of milk sample was transferred into a microcentrifuge tube and centrifuged at 10,000 × g for 5 min at 4 °C to pellet bacteria, which were then resuspended in 1 mL of sterile PBS (pH 7.4). The samples were centrifuged at 10,000 × g for 3 min, the supernatant was discarded, and this step was repeated twice. This procedure reduces milk fat and casein interference in the downstream DNA extraction.

4.9. Genomic DNA extraction

Genomic DNA extraction was completed using Promega Wizard® Genomic DNA Purification Kit (cat. No. A1120), with a few changes. A 1 mL aliquot was pelleted at 16,000 g for 5 min then resuspended in the provided nuclei lysis solution and boiled for 5 mins at 80 °C. To eliminate RNA contamination, 3 μL of RNase Solution was added to the lysate, mixed by gentle inversion, and incubated at 37 °C for 15–60 min. The sample was then allowed to cool to room temperature. Proteins were precipitated using the provided protein precipitation solution and removed via centrifuging at 16,000 g for 3 min and moving the supernatant to a 1.5 mL Eppendorf tube containing ice cold 600 μL isopropanol. Samples were then further washed with 70 % ethanol then spun down and air dried in a fume hood for 10 min. DNA pellet was rehydrated using Rehydration solution overnight at 4 °C before storage at − 20 °C.

4.10. SYBR-based real time qPCR

qPCR was performed using PowerTrack SYBR Green Mastermix (A46109, Thermo Fisher Scientific, Inc. Waltham, MA, USA), and primers were purchased from PrimeTime™ (Integrated DNA Technologies, Inc. Iowa, USA). The parameters of the designed primers were listed in **Table S5**. A standard curve for SYBR Green qPCR was conducted firstly using a tenfold dilution known concentration DNA sample. Then, four groups of 20 μL reactions with extracted DNA samples were prepared according to the standard protocol using 1 × PowerTrack™ SYBR™ Green Master Mix, 400 nM Forward and reverse primers, 2 μL target DNA, and Nuclease-free water. PCR was performed using a PTC Tempo Thermal Cycler (Bio-Rad Laboratories, Inc. California 94547, USA) in fast cycling mode, which is designed for efficient and rapid DNA amplification, particularly suitable for short amplicons. The procedure consisted of enzyme activation at 95 °C for 2 min, followed by 40 cycles of denaturation at 95 °C for 5 s. The final step in each cycle was the annealing and extension phase at 60 °C for 30 s, where primers annealed to the template and DNA polymerase synthesized the complementary strand.

5. Conclusions

In conclusion, d^{3}CRISPR presents a rapid, ultrasensitive, and high-throughput approach for the absolute quantitation of DNA molecules, without the need of target sequence amplification. Through the integration of the CRISPR/sCas12a-based nucleic acid detection system with droplet digital microfluidics, our technique demonstrates excellent sensitivity, specificity, and accuracy for target DNA quantification. The LOD for HPV 18 DNA and *E. coli* DNA was 100 aM and 60 copies/μL, respectively, representing over a 1,000-fold improvement compared to existing bulk analysis amplification-free Cas12a assays. The dynamic range for HPV DNA detection spans 5 orders of magnitude (from 10^2 aM to 5×10^5 aM), covering the natural range for DNA expression. Overall, the d^{3}CRISPR technique represents a significant advancement in nucleic acid molecular diagnostics for both research and clinical applications.

CRediT authorship contribution statement

Yang Zhang: Writing – original draft, Visualization, Validation, Software, Project administration, Methodology, Investigation, Formal analysis, Data curation. **Hangrui Liu:** Methodology. **Shi-Yang Tang:** Writing – review & editing, Funding acquisition. **Yaxiaer Yalikun:** Writing – review & editing, Funding acquisition. **Tracie J. Barber:** Writing – review & editing, Resources. **Keisuke Goda:** Writing – review & editing, Funding acquisition. **Ming Li:** Writing – review & editing, Writing – original draft, Visualization, Validation, Supervision, Resources, Project administration, Methodology, Funding acquisition, Conceptualization.

Declaration of competing interest

The authors declare that they have no known competing financial interests or personal relationships that could have appeared to influence the work reported in this paper.

Acknowledgments

This research was supported by the Australian Research Council (ARC) Discovery Project (DP200102269 and DP240100795). Ming Li is a recipient of the National Health and Medical Research Council Emerging Leadership Fellowship (GNT2017679). Yang Zhang acknowledges the financial support from Tuition Fee Scholarship (TFS) at UNSW for graduate study. **Abstract graphics**, Fig. 1, Fig. 2**a**, Fig. 3**a**, **and** Fig. 5**a** were created with BioRender.com. We sincerely appreciate Professor Ruiting Lan and Associate Professor Jai Tree from UNSW for kindly providing the biological samples used in this study. We also thank Thomas Zammit for his assistance with the DNA extraction.

Appendix A. Supplementary data

Supplementary data to this article can be found online at https://doi.org/10.1016/j.cej.2025.162098.

Data availability

Data will be made available on request.

References

[1] L.W. Koblan, M.R. Erdos, C. Wilson, W.A. Cabral, J.M. Levy, Z.-M. Xiong, U. L. Tavarez, L.M. Davison, Y.G. Gete, X. Mao, G.A. Newby, S.P. Doherty, N. Narisu, Q. Sheng, C. Krilow, C.Y. Lin, L.B. Gordon, K. Cao, F.S. Collins, J.D. Brown, D. R. Liu, In vivo base editing rescues Hutchinson–Gilford progeria syndrome in mice, Nature 589 (7843) (2021) 608–614, https://doi.org/10.1038/s41586-020-03086-7.

[2] C. Martin-Alonso, S. Tabrizi, K. Xiong, T. Blewett, S. Sridhar, A. Crnjac, S. Patel, Z. An, A. Bekdemir, D. Shea, S.-T. Wang, S. Rodriguez-Aponte, C.A. Naranjo, J. Rhoades, J.D. Kirkpatrick, H.E. Fleming, A.P. Amini, T.R. Golub, J.C. Love, S. N. Bhatia, V.A. Adalsteinsson, Priming agents transiently reduce the clearance of cell-free DNA to improve liquid biopsies, Science 383 (6680) (2024) eadf2341, https://doi.org/10.1126/science:adf2341.

[3] C. Cao, N. Cirauqui, M.J. Marcaida, E. Buglakova, A. Duperrex, A. Radenovic, M. Dal Peraro, Single-molecule sensing of peptides and nucleic acids by engineered aerolysin nanopores, Nat. Commun. 10 (1) (2019) 4918, https://doi.org/10.1038/s41467-019-12690-9.

[4] M. Tayyab, D. Barrett, G. van Riel, S. Liu, B. Reinius, C. Scharfe, P. Griffin, L. M. Steinmetz, M. Javanmard, V. Pelechano, Digital assay for rapid electronic quantification of clinical pathogens using DNA nanoballs, Sci. Adv. 9 (36) (2023) eadi4997, https://doi.org/10.1126/sciadv.adi4997.

[5] J. Yan, R. Bhadane, M. Ran, X. Ma, Y. Li, D. Zheng, O.M.H. Salo-Ahen, H. Zhang, Development of Aptamer-DNAzyme based metal-nucleic acid frameworks for gastric cancer therapy, Nat. Commun. 15 (1) (2024) 3684, https://doi.org/10.1038/s41467-024-48149-9.

[6] B. Chen, Y. Jiang, X. Cao, C. Liu, N. Zhang, D. Shi, Droplet digital PCR as an emerging tool in detecting pathogens nucleic acids in infectious diseases, Clin. Chim. Acta 517 (2021) 156–161, https://doi.org/10.1016/j.cca.2021.02.008.

[7] S. Chen, Y. Sun, F. Fan, S. Chen, Y. Zhang, Y. Zhang, X. Meng, J.-M. Lin, Present status of microfluidic PCR chip in nucleic acid detection and future perspective, TrAC Trends Anal. Chem. 157 (2022) 116737, https://doi.org/10.1016/j.trac.2022.116737.

[8] S. Olmedillas-López, R. Olivera-Salazar, M. García-Arranz, D. García-Olmo, Current and Emerging Applications of Droplet Digital PCR in Oncology: An Updated Review, Mol. Diagn. Ther. 26 (1) (2022) 61–87, https://doi.org/10.1007/s40291-021-00562-2.

[9] A.T. Xiao, Y.X. Tong, S. Zhang, False negative of RT-PCR and prolonged nucleic acid conversion in COVID-19: Rather than recurrence, J. Med. Virol. 92 (10) (2020) 1755–1756, https://doi.org/10.1002/jmv.25855.

[10] L. Becherer, N. Borst, M. Bakheit, S. Frischmann, R. Zengerle, F. von Stetten, Loop-mediated isothermal amplification (LAMP) – review and classification of methods for sequence-specific detection, Anal. Methods 12 (6) (2020) 717–746, https://doi.org/10.1039/C9AY02246E.

[11] J. Zhang, Y. Fan, J. Li, B. Huang, H. Wen, J. Ren, Cascade signal enhancement by integrating DNA walking and RCA reaction-assisted "silver-link" crossing electrode for ultrasensitive electrochemical detection of Staphylococcus aureus, Biosensors Bioelectron. 217 (2022) 114716, https://doi.org/10.1016/j.bios.2022.114716.

[12] I. Seder, R. Coronel-Tellez, S.H. Helalat, Y. Sun, Fully integrated sample-in-answer-out platform for viral detection using digital reverse transcription recombinase polymerase amplification (dRT-RPA), Biosensors Bioelectron. 237 (2023) 115487, https://doi.org/10.1016/j.bios.2023.115487.

[13] J. Qian, S.A. Boswell, C. Chidley, Z.-X. Lu, M.E. Pettit, B.L. Gaudio, J.M. Fajnzylber, R.T. Ingram, R.H. Ward, J.Z. Li, M. Springer, An enhanced isothermal amplification assay for viral detection, Nat. Commun. 11 (1) (2020) 5920, https://doi.org/10.1038/s41467-020-19258-y.

[14] E.A. Pumford, J. Lu, I. Spaczai, M.E. Prasetyo, E.M. Zheng, H. Zhang, D.T. Kamei, Developments in integrating nucleic acid isothermal amplification and detection systems for point-of-care diagnostics, Biosensors Bioelectron. 170 (2020) 112674, https://doi.org/10.1016/j.bios.2020.112674.

[15] M.S. Lowenthal, E. Quittman, K.W. Phinney, Absolute Quantification of RNA or DNA Using Acid Hydrolysis and Mass Spectrometry, Anal. Chem. 91 (22) (2019) 14569–14576, https://doi.org/10.1021/acs.analchem.9b03625.

[16] Y. Pang, Q. Li, C. Wang, S. zhen, Z. Sun, R. Xiao, CRISPR-Cas12a mediated SERS lateral flow assay for amplification-free detection of double-stranded DNA and single-base mutation, Chem. Eng. J. 429 (2022) 132109, https://doi.org/10.1016/j.cej.2021.132109.

[17] L. Lin, J. Song, Y. Du, Q. Wu, J. Gao, Y. Song, C. Yang, W. Wang, Quantification of Bacterial metabolic activities in the gut by d-amino acid-based invivo labeling, Angew. Chem. Int. Ed. 59 (29) (2020) 11923–11926, https://doi.org/10.1002/anie.202004703.

[18] Y. Chen, C. Qian, C. Liu, H. Shen, Z. Wang, J. Ping, J. Wu, H. Chen, Nucleic acid amplification free biosensors for pathogen detection, Biosensors Bioelectron. 153 (2020) 112049, https://doi.org/10.1016/j.bios.2020.112049.

[19] X. Li, X. Yang, Z. Pan, S. Zhuo, Z. Lin, J. Chen, Nucleic acid amplification-free biosensor for sensitive and specific cfDNA detection based on CRISPR-Cas12a and single nanoparticle dark-field microscopy (DFM) imaging, Sensors Actuators b: Chem. 406 (2024) 135363, https://doi.org/10.1016/j.snb.2024.135363.

[20] J.A. Kulkarni, D. Witzigmann, S.B. Thomson, S. Chen, B.R. Leavitt, P.R. Cullis, R. van der Meel, The current landscape of nucleic acid therapeutics, Nat. Nanotechnol. 16 (6) (2021) 630–643, https://doi.org/10.1038/s41565-021-00898-0.

[21] J.Y. Wang, J.A. Doudna, CRISPR technology: A decade of genome editing is only the beginning, Science 379 (6629) (2023) eadd8643, https://doi.org/10.1126/science:add8643.

[22] S.-Y. Li, Q.-X. Cheng, J.-K. Liu, X.-Q. Nie, G.-P. Zhao, J. Wang, CRISPR-Cas12a has both cis-and trans-cleavage activities on single-stranded DNA, Cell Res. 28 (4) (2018) 491–493.

[23] Y. Wang, Y. Ke, W. Liu, Y. Sun, X. Ding, A One-Pot Toolbox Based on Cas12a/crRNA Enables Rapid Foodborne Pathogen Detection at Attomolar Level, ACS Sensors 5 (5) (2020) 1427–1435, https://doi.org/10.1021/acssensors.0c00320.

[24] J.S. Gootenberg, O.O. Abudayyeh, J.W. Lee, P. Essletzbichler, A.J. Dy, J. Joung, V. Verdine, N. Donghia, N.M. Daringer, C.A. Freije, Nucleic acid detection with CRISPR-Cas13a/C2c2, Science 356 (6336) (2017) 438–442.

[25] Y. Hou, S. Chen, Y. Zheng, X. Zheng, J.-M. Lin, Droplet-based digital PCR (ddPCR) and its applications, TrAC Trends Anal. Chem. 158 (2023) 116897, https://doi.org/10.1016/j.trac.2022.116897.

[26] P. Fozouni, S. Son, M. Díaz León Derby, G.J. Knott, C.N. Gray, M.V. D'Ambrosio, C. Zhao, N.A. Switz, G.R. Kumar, S.I. Stephens, D. Boehm, C.-L. Tsou, J. Shu, A. Bhuiya, M. Armstrong, A.R. Harris, P.-Y. Chen, J.M. Osterloh, A. Meyer-Franke, B. Joehnk, K. Walcott, A. Sil, C. Langelier, K.S. Pollard, E.D. Crawford, A. S. Puschnik, M. Phelps, A. Kistler, J.L. DeRisi, J.A. Doudna, D.A. Fletcher, M. Ott, Amplification-free detection of SARS-CoV-2 with CRISPR-Cas13a and mobile phone microscopy, Cell 184 (2) (2021) 323–333, https://doi.org/10.1016/j.cell.2020.12.001.

[27] H. Altae-Tran, S. Kannan, A.J. Suberski, K.S. Mears, F.E. Demircioglu, L. Moeller, S. Kocalar, R. Oshiro, K.S. Makarova, R.K. Macrae, E.V. Koonin, F. Zhang, Uncovering the functional diversity of rare CRISPR-Cas systems with deep terascale clustering, Science 382 (6673) (2023) eadi1910, https://doi.org/10.1126/science:adi1910.

[28] T. Tian, B.W. Shu, Y.Z. Jiang, M.M. Ye, L. Liu, Z.H. Guo, Z.P. Han, Z. Wang, X. M. Zhou, An Ultralocalized Cas13a Assay Enables Universal and Nucleic Acid Amplification-Free Single-Molecule RNA Diagnostics, ACS Nano 15 (1) (2021) 1167–1178, https://doi.org/10.1021/acsnano.0c08165.

[29] H. Yue, B. Shu, T. Tian, E. Xiong, M. Huang, D. Zhu, J. Sun, Q. Liu, S. Wang, Y. Li, X. Zhou, Droplet Cas12a assay enables DNA quantification from unamplified samples at the single-molecule level, Nano Lett. 21 (11) (2021) 4643–4653, https://doi.org/10.1021/acs.nanolett.1c00715.

[30] H. Wu, X. Cao, Y. Meng, D. Richards, J. Wu, Z. Ye, A.J. deMello, DropCRISPR: a LAMP-Cas12a-based digital method for ultrasensitive detection of nucleic acid, Biosens. Bioelectron 211 (2022) 114377, https://doi.org/10.1016/j.bios.2022.114377.

[31] X. Wu, C. Chan, S.L. Springs, Y.H. Lee, T.K. Lu, H. Yu, A warm-start digital CRISPR/Cas-based method for the quantitative detection of nucleic acids, Anal. Chim. Acta 1196 (2022) 339494, https://doi.org/10.1016/j.aca.2022.339494.

[32] Y. Zhou, J. Zhao, R. Chen, P. Lu, W. Zhao, R. Ma, T. Xiao, Y. Dong, W. Zheng, X. Huang, B.Z. Tang, Y. Chen, A portable deep-learning-assisted digital single-particle counting biosensing platform for amplification-free nucleic acid detection using a lens-free holography microscope, Nano Today 56 (2024) 102238, https://doi.org/10.1016/j.nantod.2024.102238.

[33] Y. Zhou, J. Zhao, J. Wen, Z. Wu, Y. Dong, Y. Chen, Unsupervised learning-assisted acoustic-driven nano-lens holography for the ultrasensitive and amplification-free detection of viable bacteria, Adv. Sci. 12 (2) (2025) 2406912, https://doi.org/10.1002/advs.202406912.

[34] T.W. Cowell, A. Dobria, H.-S. Han, Simplified, Shear Induced Generation of Double Emulsions for Robust Compartmentalization during Single Genome Analysis, ACS Appl. Mater. Interfaces 14 (18) (2022) 20528–20537, https://doi.org/10.1021/acsami.1c22692.

[35] Y. Li, S. Li, J. Wang, G. Liu, CRISPR/Cas systems towards next-generation biosensing, Trends Biotechnol. 37 (7) (2019) 730–743, https://doi.org/10.1016/j.tibtech.2018.12.005.

[36] Y. Zhang, H. Liu, Y. Nakagawa, Y. Nagasaka, T. Ding, S.-Y. Tang, Y. Yalikun, K. Goda, M. Li, Enhanced CRISPR/Cas12a-based quantitative detection of nucleic acids using double emulsion droplets, Biosensors Bioelectron. 257 (2024) 116339, https://doi.org/10.1016/j.bios.2024.116339.
[37] K.K. Brower, M. Khariton, P.H. Suzuki, C. Still 2nd, G. Kim, S.G.K. Calhoun, L.S. Qi, B. Wang, P.M. Fordyce, Double emulsion picoreactors for high-throughput single-cell encapsulation and phenotyping via FACS, Anal Chem 92 (19) (2020) 13262–13270, https://doi.org/10.1021/acs.analchem.0c02499.
[38] K.K. Brower, C. Carswell-Crumpton, S. Klemm, B. Cruz, G. Kim, S.G.K. Calhoun, L. Nichols, P.M. Fordyce, Double emulsion flow cytometry with high-throughput single droplet isolation and nucleic acid recovery, Lab Chip 20 (12) (2020) 2062–2074, https://doi.org/10.1039/d0lc00261e.
[39] H. Liu, J.A. Piper, M. Li, Rapid, simple, and inexpensive spatial patterning of wettability in microfluidic devices for double emulsion generation, Anal. Chem. 93 (31) (2021) 10955–10965, https://doi.org/10.1021/acs.analchem.1c01861.
[40] T. Cowell, H.-S. Han, Double emulsion flow cytometry for rapid single genome detection, in: Single-Cell Assays: Microfluidics, Genomics, and Drug Discovery, Springer, 2023, pp. 155–167.
[41] L. Vermeir, P. Sabatino, M. Balcaen, A. Declerck, K. Dewettinck, J.C. Martins, G. Guthausen, P. Van der Meeren, Effect of molecular exchange on water droplet size analysis as determined by diffusion NMR: The W/O/W double emulsion case, J. Colloid Interface Sci. 475 (2016) 57–65, https://doi.org/10.1016/j.jcis.2016.04.029.
[42] J.-K. Guo, H. Wang, F. Chang, J. Ling, Y. Yuan, X. Zhang, X. Wang, Production and reconfiguration of double emulsions by temperature control, Langmuir 39 (37) (2023) 13296–13302, https://doi.org/10.1021/acs.langmuir.3c01891.
[43] M. Rossetti, R. Merlo, N. Bagheri, D. Moscone, A. Valenti, A. Saha, P.R. Arantes, R. Ippodrino, F. Ricci, I. Treglia, E. Delibato, J. Oost, G. Palermo, G. Perugino, A. Porchetta, Enhancement of CRISPR/Cas12a trans-cleavage activity using hairpin DNA reporters, Nucleic Acids Res. 50 (14) (2022) 8377–8391, https://doi.org/10.1093/nar/gkac578.
[44] A.B. Pebdeni, A. Roshani, E. Mirsadoughi, S. Behzadifar, M. Hosseini, Recent advances in optical biosensors for specific detection of E. coli bacteria in food and water, Food Control 135 (2022) 108822, https://doi.org/10.1016/j.foodcont.2022.108822.
[45] J. Wang, S. Hahn, E. Amstad, N. Vogel, Tailored double emulsions made simple, Adv. Mater. 34 (5) (2022) 2107338, https://doi.org/10.1002/adma.202107338.
[46] Z. Zhu, F. Huang, C. Yang, T. Si, R.X. Xu, On-demand generation of double emulsions based on interface shearing for controlled ultrasound activation, ACS Appl. Mater. Interfaces 11 (43) (2019) 40932–40943, https://doi.org/10.1021/acsami.9b15182.
[47] J.M. Perkel, LIFE SCIENCE TECHNOLOGIES: EBB AND FLOW: Cytometry for the next generation, Science 330 (6005) (2010) 853, https://doi.org/10.1126/science:330.6005.853.
[48] H. Xu, A. Xia, D. Wang, Y. Zhang, S. Deng, W. Lu, J. Luo, Q. Zhong, F. Zhang, L. Zhou, W. Zhang, Y. Wang, C. Yang, K. Chang, W. Fu, J. Cui, M. Gan, D. Luo, M. Chen, An ultraportable and versatile point-of-care DNA testing platform, Sci. Adv. 6 (17) (2020) eaaz7445, https://doi.org/10.1126/sciadv.aaz7445.
[49] P.-C. Chen, J. Lawrensen, Improving a smartphone based droplet flow cytometry system with micro lens arrays integrated optofluidic chip, Sens. Actuators, A 367 (2024) 115080, https://doi.org/10.1016/j.sna.2024.115080.
[50] J. Son, B. Mandracchia, A.D. Silva Trenkle, G.A. Kwong, S. Jia, Portable light-sheet optofluidic microscopy for 3D fluorescence imaging flow cytometry, Lab Chip 23 (4) (2023) 624–630, https://doi.org/10.1039/D2LC01024K.
[51] I.C. Clark, M.A. Wheeler, H.-G. Lee, Z. Li, L.M. Sanmarco, S. Thaploo, C.M. Polonio, S.W. Shin, G. Scalisi, A.R. Henry, J.M. Rone, F. Giovannoni, M. Charabati, C.F. Akl, D.M. Aleman, S.E.J. Zandee, A. Prat, D.C. Douek, E.A. Boritz, F.J. Quintana, A. R. Abate, Identification of astrocyte regulators by nucleic acid cytometry, Nature 614 (7947) (2023) 326–333, https://doi.org/10.1038/s41586-022-05613-0.